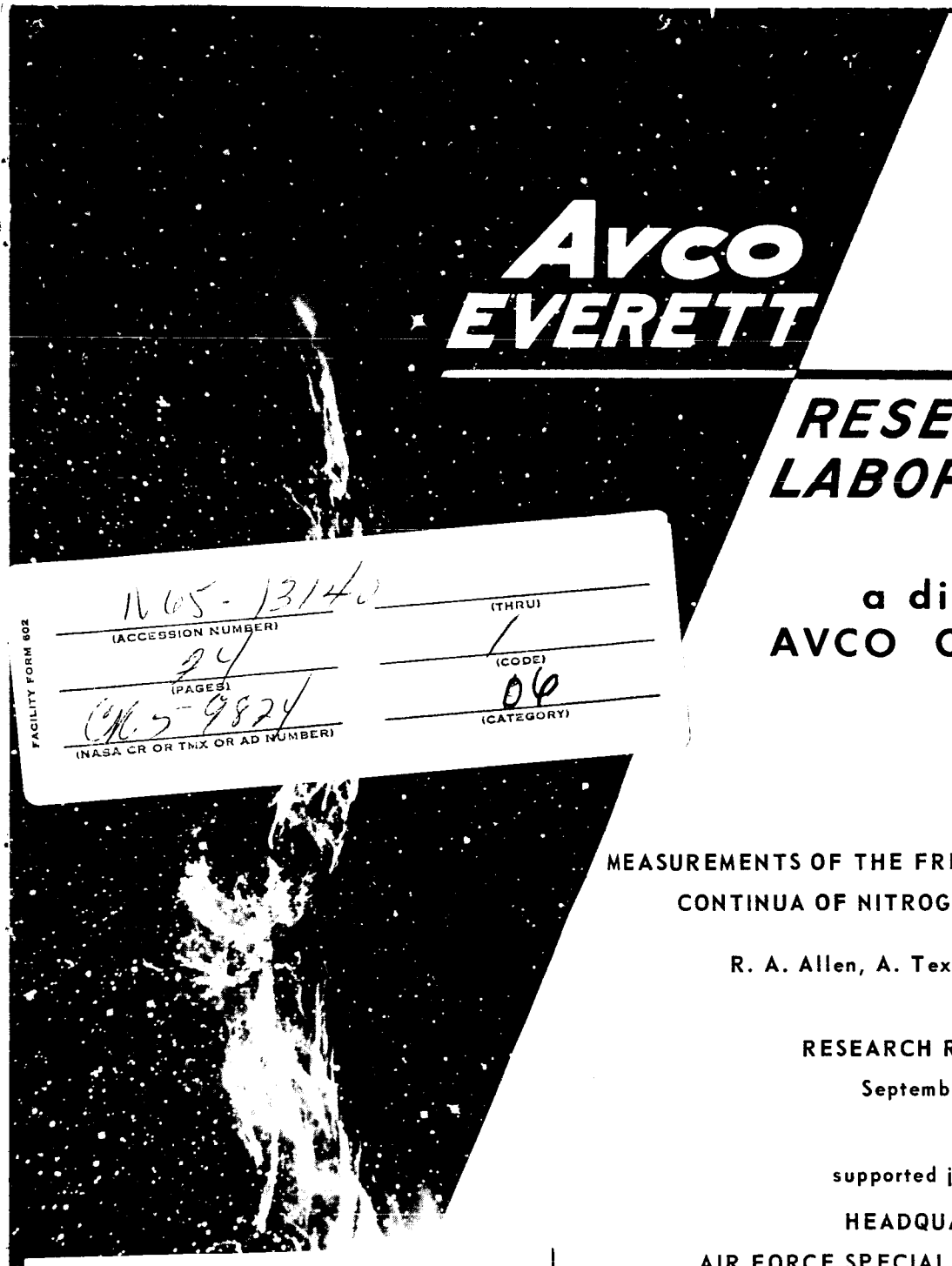

AVCO EVERETT RESEARCH LABORATORY

a division of
AVCO CORPORATION

MEASUREMENTS OF THE FREE-BOUND AND FREE-FREE CONTINUA OF NITROGEN, OXYGEN AND AIR

R. A. Allen, A. Textoris and J. Wilson

RESEARCH REPORT 195
September 1964

supported jointly by
HEADQUARTERS
AIR FORCE SPECIAL WEAPONS CENTER
AIR FORCE SYSTEMS COMMAND
UNITED STATES AIR FORCE
Kirtland Air Force Base, New Mexico
under Contract No. AF 29(601)-6488
Project No. 7811

HEADQUARTERS
NATIONAL AERONAUTICS AND SPACE ADMINISTRATION
OFFICE OF ADVANCED RESEARCH AND TECHNOLOGY
Washington 25, D. C.
under Contract No. NAS w-748

RESEARCH REPORT 195

MEASUREMENTS OF THE FREE-BOUND AND FREE-FREE CONTINUA OF NITROGEN, OXYGEN AND AIR

by

R. A. Allen, A. Textoris and J. Wilson

AVCO-EVERETT RESEARCH LABORATORY
a division of
AVCO CORPORATION
Everett, Massachusetts

September 1964

supported jointly by

HEADQUARTERS
AIR FORCE SPECIAL WEAPONS CENTER
AIR FORCE SYSTEMS COMMAND
UNITED STATES AIR FORCE
Kirtland Air Force Base, New Mexico

under Contract No. AF 29(601)-6488

Project No. 7811

HEADQUARTERS
NATIONAL AERONAUTICS AND SPACE ADMINISTRATION
OFFICE OF ADVANCED RESEARCH AND TECHNOLOGY
Washington 25, D. C.

under Contract No. NAS w-748

ABSTRACT

13140

Measurements have been made of the equilibrium radiation behind incident and reflected shocks produced in an electric arc-driven shock tube over a temperature range of 8000-14, 000°K. Experiments are described which used a tungsten photoelectric gauge to make photometric measurements in the vacuum ultraviolet. This gauge was positioned at the axis of the shock tube and cored the oncoming shock wave. By the use of optical stops, this gauge was capable of resolving the shock front. A knowledge of the photoelectric yield of the tungsten provided a photometric measurement. The photoionization cross section for the ground state nitrogen atom was inferred from these measurements to be of the order of $10^{-17} cm^2$.

Data were also obtained of the continua at .51μ in nitrogen, oxygen and air which gave information on the component of the radiation produced by electrons being captured by ions and neutral atoms. The measurements agree well with free-bound calculations assuming a hydrogen-like model for N and O.

Measurements were also obtained in the infrared at 6.1μ in air over a range of shock conditions which infer a product of an effective Z^2 and Gaunt factor of 1.5 for the air constituent free-free transitions.

author

I. INTRODUCTION

Three types of photometric measurements will be described. They were made in order to examine the continuum radiation emitted from high temperature air and its constituent gases produced in the equilibrium region behind incident and reflected shock waves. The measurements cover three regions of the spectra and were made using three different measuring techniques. A newly developed tungsten gauge was used to make measurements in the vacuum ultraviolet. Photomultipliers in conjunction with a monochromator were used for the visible region of the spectra and a gold doped germanium infrared cell with a filter was used for the infrared measurements. The free-bound and the wings of bound-bound electronic transitions contribute the most to the continuum radiation from plasmas in the vacuum ultraviolet and the visible, while the free-free transition is the dominant radiating mechanism in the far infrared. In polyelectronic atoms, excitation and ionization by photons from the ground state and near ground state levels are most likely not to be hydrogen-like and, consequently, much more difficult to calculate. For the nitrogen and oxygen atom, these transitions occur at wavelengths shorter than 2000 Å. For this reason, photometric measurements of high temperature air in the vacuum ultraviolet are invaluable in checking theoretical predictions.

The experiments were carried out on electric arc-heated shock tubes of 1.5 and 6-inch diameters. The operation of these shock tubes is well documented[1] and will not be discussed in the present paper. In order to obtain measurements over a wide range of densities, measurements were made using reflected as well as incident shock waves.

II. TUNGSTEN GAUGE MEASUREMENTS

Experimental

A diagram of the tungsten photoelectric gauge is shown in Fig. 1. It consists of a cylinder concentric with an outer sleeve, positioned at the axis of the shock tube such that it cored the oncoming shock wave. The diameter of the inside cylinder was 5 cm and the inside diameter of the outside sleeve, 8.8 cm. The viewing solid angle of the gauge was determined by the slit spacing which was .635 mm. This corresponds to a spatial resolution of the gauge of 1.4 mm for an optical path length of 1.93 cm. The tungsten photosensing surface was in the form of a 1.85 cm diameter ring and was cleaned prior to each run using an electric current and a sodium hydroxide solution. In making shock tube runs, the output signal was fed to an oscilloscope and the traces were photographed. The output signal was found to be independent of the voltage on the gauge between 15 and 30 volts and indicated that the gauge operated as a photocell. As a further check to insure that the detector was operating as a vacuum UV photocell, a quartz sleeve was inserted over the photosensing surface for several runs. The quartz sleeve was found, as expected, to eliminate the output signal. Also a test was made to insure that the signal was not that produced by space charge effects in the cavity within the gauge. A fine wire mesh sleeve attached to ground was inserted over a tungsten ring. This was found to reduce the output signal only by the amount corresponding to the geometric reduction of the surface area viewing the signal. In the operation of the gauge, the path length could be varied between 1.93 cm and 5.1 cm by removing the outer sleeve.

Typical oscillograms obtained from incident air shocks at an initial pressure of 0.2 mm Hg are shown in Fig. 2. The tungsten gauge signal is on the bottom with time moving from left to right. The top traces in the figure are those produced by a photomultiplier sensitive in the visible and was used to locate the shock front as well as provide the last signal for a three station speed measuring system. The test time on the tungsten gauge signal was about 4 μsec and corresponds to the time for the hot test gas to diffuse to the tungsten surface. Data from two runs at two different shock speeds show how the character of the tungsten gauge signal changes for a small increase in velocity. The voltage setting of the oscilloscope on the bottom trace for both measurements was the same. The equilibrium level was taken as the level region immediately behind the radiative relaxation region. The steps in the radiative relaxation region of the tungsten gauge are unexplained. Further tests are needed to determine whether or not they are a real effect in the gas.

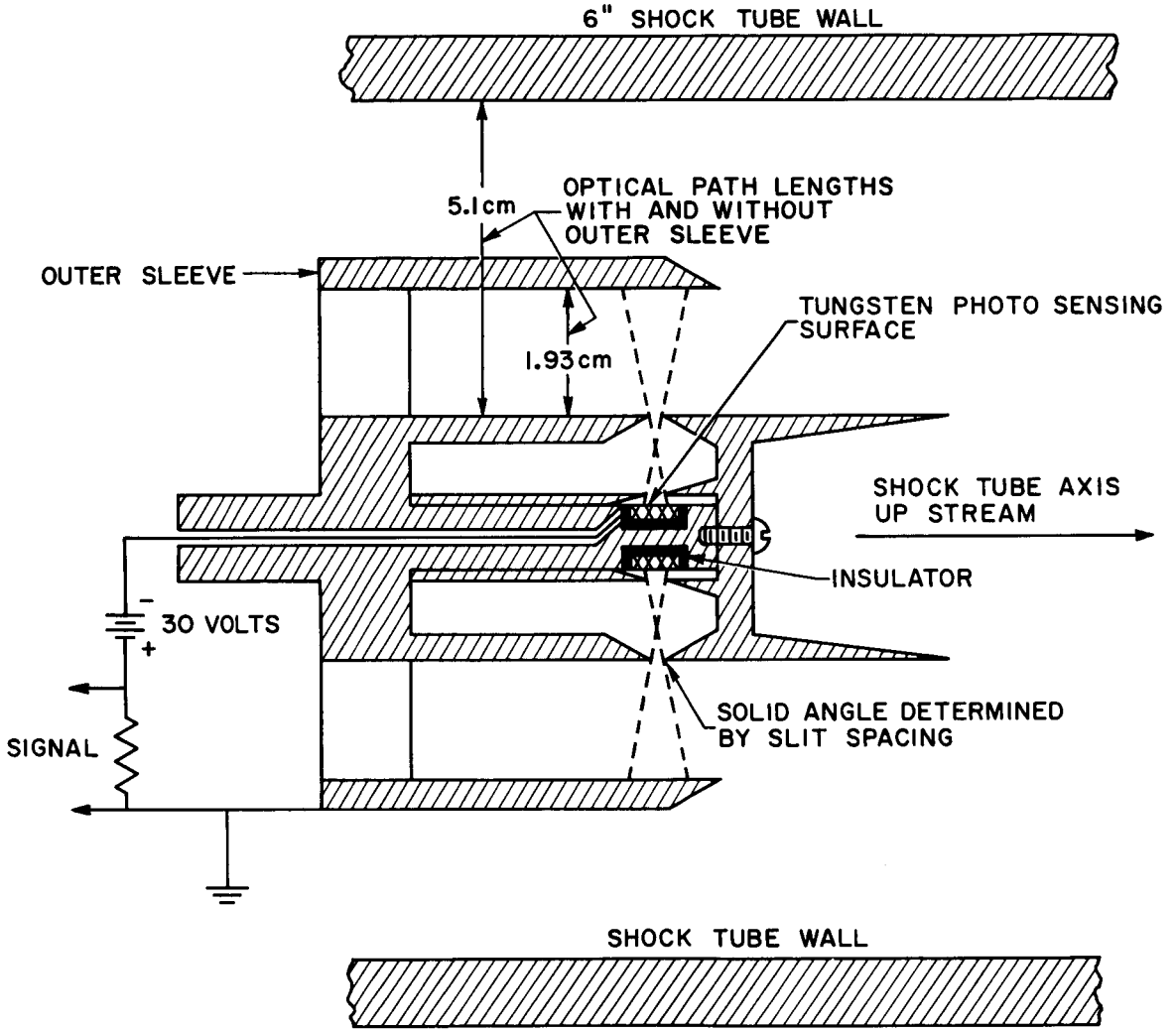

Fig. 1 Schematic diagram of tungsten photoelectric gauge used to make photometric measurements in the vacuum ultraviolet.

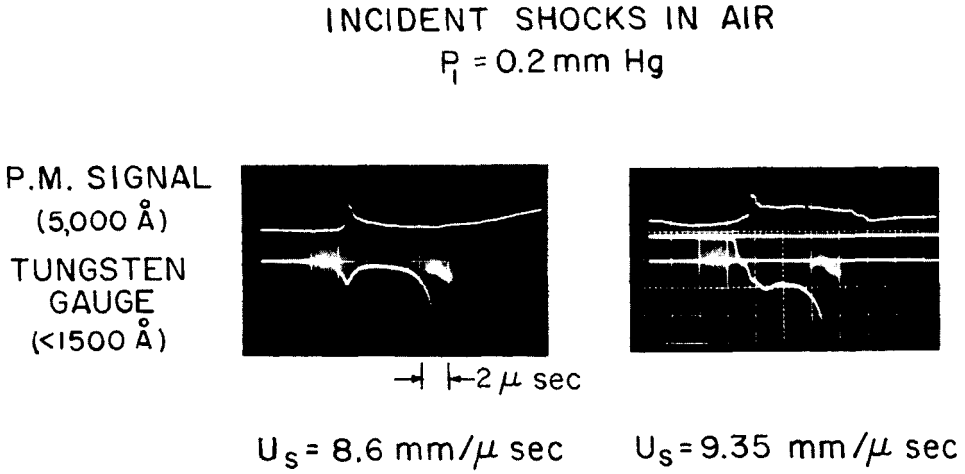

Fig. 2 Typical data obtained with the tungsten photoelectric gauge. The upper trace is the signal from a photomultiplier indicating the location of the shock front.

Equilibrium air data from the tungsten gauge are displayed in Fig. 3 versus shock speed for an initial pressure of 0.2 mm Hg. Measurements were made at two path lengths. The initial shock conditions are used to calculate the equilibrium temperatures displayed at the top of the figure. The analysis of this data will now be discussed.

Black Body Considerations

In order to analyze the tungsten gauge data shown in Fig. 3, several approaches can be made. One of the immediate ways is to examine how the signal changes with path length. The data between 9 and 10 mm/μsec changes by a factor of roughly 2.0 for a path length change of a factor of 2.64 indicating that the gas is partially black over the wavelength response of the gauge in this velocity range. The two data points in the vicinity of 8.5 mm/μsec indicate that the gas is essentially black at a path length of 1.93 cm, however more data points are needed at the lower velocities to improve the statistics.

A second approach to the analysis is to calculate the expected signal from the gauge and compare it with the measured value as a function of shock speed and path length. The calculation of the expected signal is accomplished by using the photoefficiencies measured for tungsten by Weissler,[2] and folding with it the expected radiation from the gas taking into account the viewing solid angle and the viewing surface area for the gauge. This latter quantity was calculated to be 1.88×10^{-2} cm^2 ster for the gauge with a .635 mm slit spacing. If the gas is assumed to be black over the total band pass of the gauge, the expected signal is that depicted in Fig. 3 by the upper dashed curve. If the integration is carried out to 1000 Å, the bottom dashed curve is produced. For these expected signals, no correction is made for the absorption of the radiation in the gas present in the cavity of the gauge. The initial pressure, P_1, was 0.2 mm Hg corresponding to 10^{16} molecules over the 1.58 cm between the tungsten surface and the entrance slit of the gauge. Assuming a photoabsorption cross section no larger than a 10^{-17} cm^2 per molecule over the band pass of the gauge, one infers no more than 9% absorption of the light in passage from the entrance slit to the tungsten surface. Since the O_2 molecule will do most of the absorbing in air,[3] this absorption loss is probably only a few percent. For this reason, absorption losses in the gauge have been neglected in the analysis of the data.

Theoretical curves for the contributions to the signal from the N_2 Birge-Hopfield system and the free-bound radiation from N^+ and O^+ are shown in Fig. 3 and will now be discussed.

Birge-Hopfield System of N_2

Wray[4] has made absorption measurements in nitrogen from which an electronic transition moment can be inferred for the Birge-Hopfield system. His measurements were made at 1270 Å with a 5 Å band pass in pure nitrogen shocks. In order to arrive at an oscillator strength from his measurements, the spectral distribution of the emission for the Birge-Hopfield system was calculated for various temperatures, assuming an electronic transition moment which was independent of wavelength.

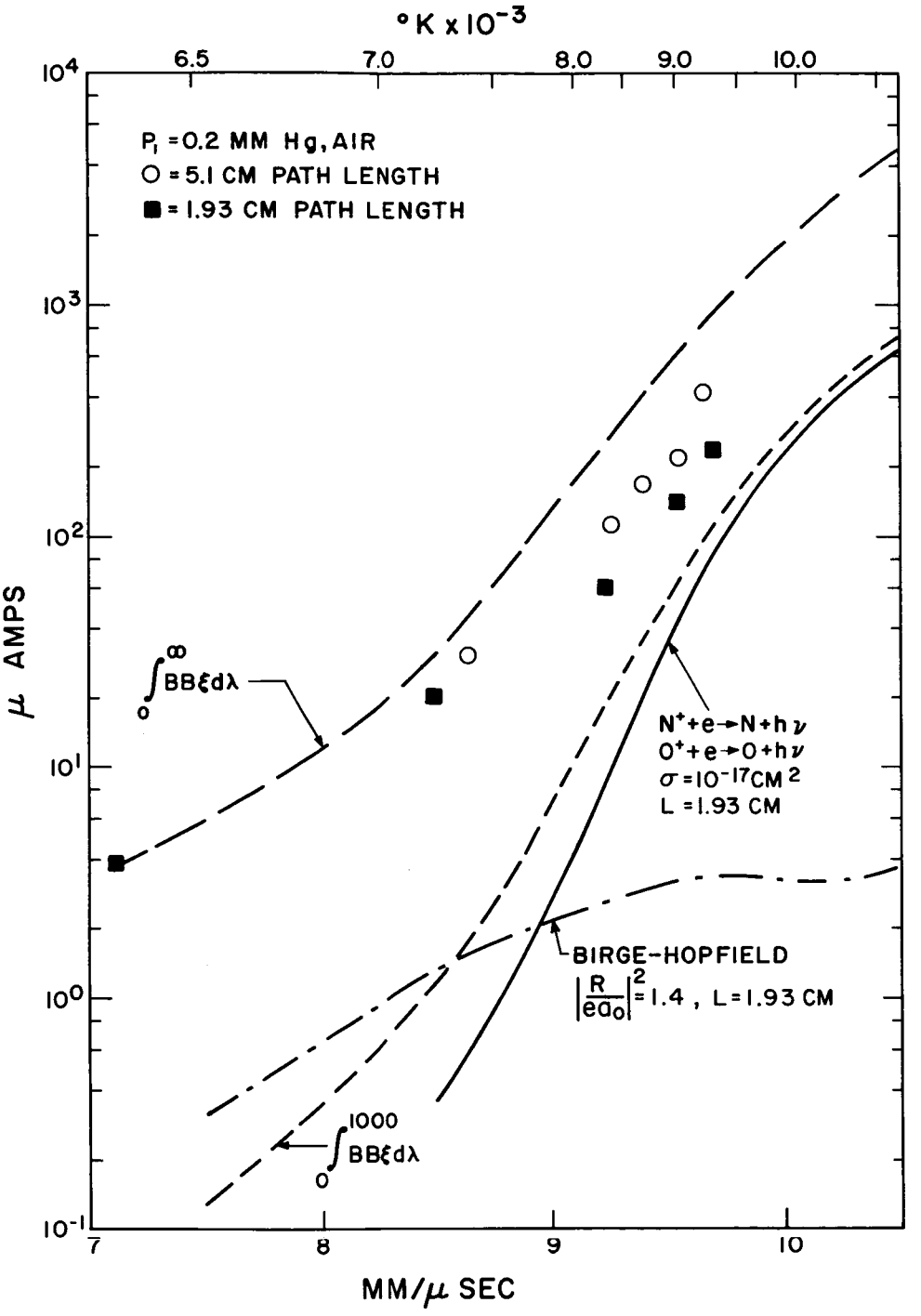

Fig. 3 Equilibrium data obtained by the photoelectric gauge from incident air shocks for two conditions of path length.

The detail of the molecular structure versus wavelength using the $\Delta J=0$ approximation and a smeared rotational line model at a given temperature is given by a parameter $\phi\lambda^{-6}$. The parameter ϕ is thoroughly described in Refs. 5, 6, 7 and 8. The inputs that make up ϕ are Franck-Condon factors and the spectroscopic constants. The spectroscopic constants used for the Birge-Hopfield system were those of Wilkinson and Houk[9] and the Franck-Condon factors were those provided by Spindler of Avco/RAD.

A computer program[7] has been developed which calculates and machine plots $\phi\lambda^{-6}$ versus wavelength. The results are shown for the Birge-Hopfield system at 10,000°K in Fig. 4. The vibrational transitions are distributed over many levels and the resultant wavelength distribution of the radiation was for practical purposes regarded as a continuum. A smooth curve was drawn through the points such as those shown in Fig. 4 for three different temperatures, and then $\phi\lambda^{-6}$ was used to calculate the absorption cross section per N_2 molecule normalized to the 7000°K absorption measurements of Wray. The results are shown in Fig. 5 and imply an electronic transition moment $\left|\frac{R}{e\,a_o}\right|^2$ of 1.4. The assumption that the Birge-Hopfield system was the dominant absorber in the measurements of Wray is indicated by the fact that the theory predicts the proper temperature dependence. This can be seen by the comparison of the 10,000°K data and theory in Fig. 5. By using these results, the theory line in Fig. 3 for the Birge-Hopfield system was constructed for a path length of 1.93 cm.

N^+ and O^+ Free-Bound Radiation

Bates and Seaton[10] have made a quantum mechanical calculation for the photoionization cross section from the ground state of the nitrogen atom of approximately $10^{-17}cm^2$ with a weak wavelength dependence over the continuum. This same cross section was used for the oxygen ground state. For the purposes of the analysis of the tungsten gauge data, this photoionization cross section with no wavelength dependence for the 2p states of N and O was used to infer the radiation to be expected from N^+ and O^+ free-bound transitions in the vacuum ultraviolet. A calculation of the free-bound contributions to the radiation and the photosensitivity of the tungsten gauge[2] are shown in Fig. 6 for a shock speed of 9.76 mm/μsec, initial pressure of 0.2 mm Hg, and a path length of 1.93 cm. The energy levels of Moore[11] were used to locate the absorption edges. Three 2p photoabsorption edges of nitrogen contribute to the radiation in the range of sensitivity of the tungsten gauge. However, only one of the 2p states of the oxygen atom contributes, since photoabsorption from the ^1D and ^1S states to produce the O^+ ion in the ^4S ground state does not conserve electron spin.

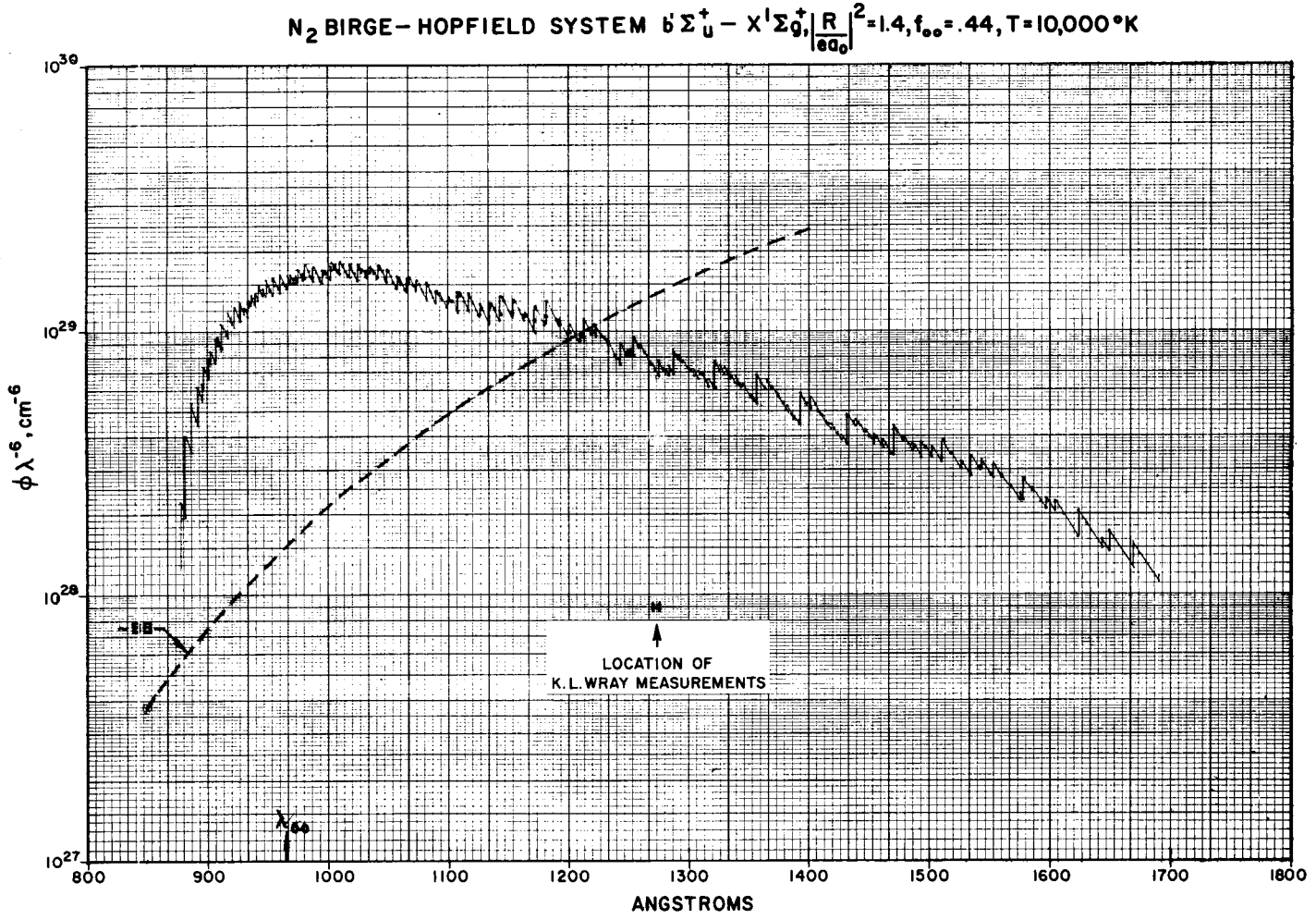

Fig. 4 The spectral distribution of the radiation intensity emitted from the N_2 Birge-Hopfield system at 10,000°K assuming an electronic transition moment independent of internuclear separation.

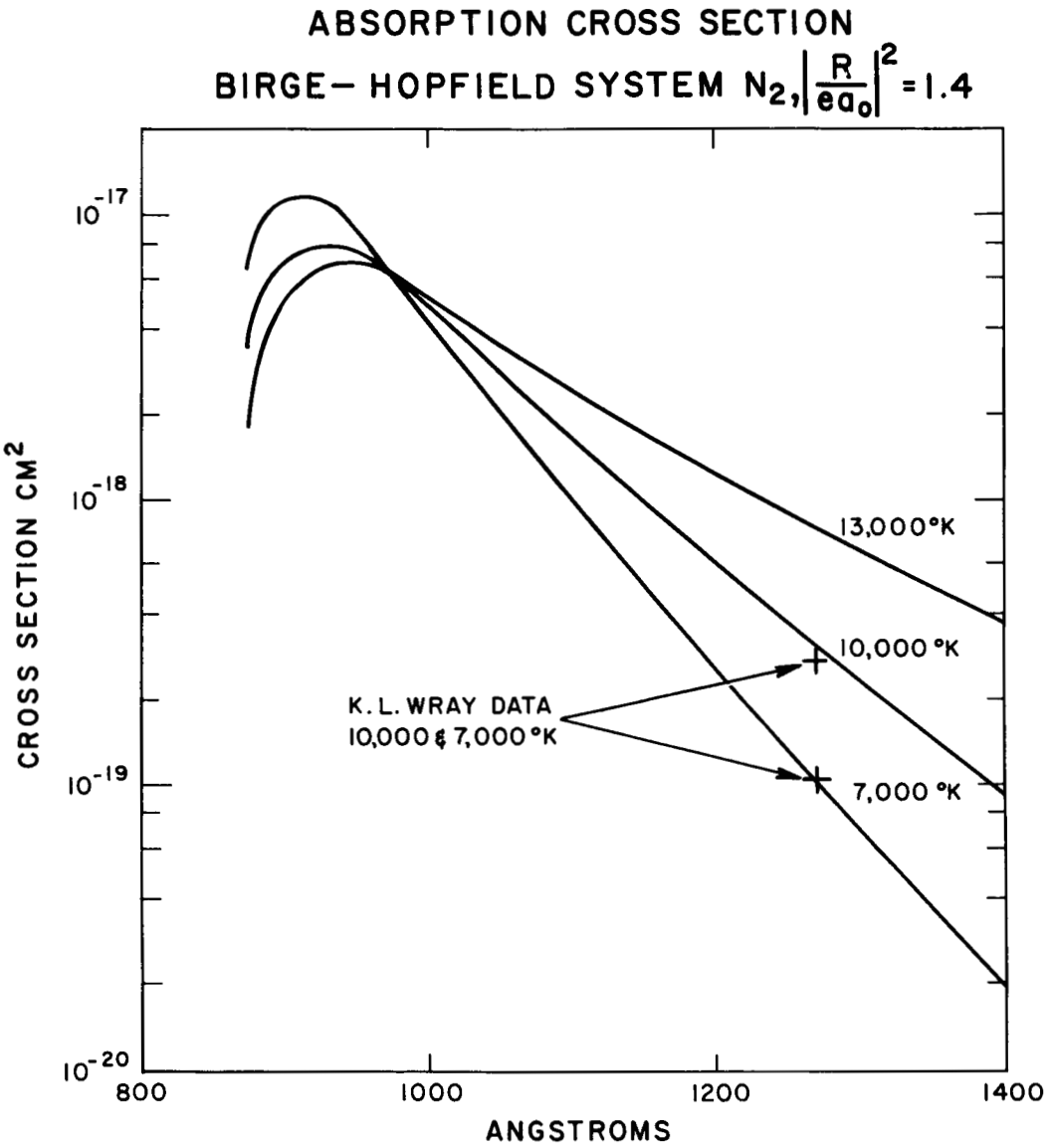

Fig. 5 Absorption coefficient per N_2 molecule for the Birge-Hopfield system for three different temperatures.

A2732

The species concentrations for this shock condition are calculated to be

$$O = 4.5 \times 10^{16} cm^{-3}, \quad N = 1.62 \times 10^{17} cm^{-3}$$
$$N_2 = 3.46 \times 10^{14} cm^{-3}, \quad e = 6.47 \times 10^{15} cm^{-3}$$

The theory of Inglis and Teller[12] was used to calculate the region over which the lines near the photoabsorption edges are merged. These regions are shaded in Fig. 6.

Also shown in the figure is the contribution to be expected from the N_2 Lyman-Birge-Hopfield system. A spectral distribution calculation was also carried out for the Lyman-Birge-Hopfield system using the Franck-Condon factors of Nicholls.[13] This radiating system is plotted in Fig. 6 using an electronic transition moment of 1.0. This value for the electronic transition moment is probably high and the system is plotted merely to show its possible contribution to the radiation.

As indicated in the figure by the dotted photoabsorption edge which extends above the black body limit, part of the spectrum is expected to be cut off by the black body limit, while regions at longer wavelength are becoming thin. Other than the merged regions in Fig. 6, no estimates are made of the contributions from bound-bound transitions. With the analysis such as that shown in Fig. 6, the expected signal from the N^+ and O^+ free-bound transitions are plotted in Fig. 3 for a 1.93 cm path length.

Concluding Remarks on Tungsten Gauge Measurements

The predicted values over the whole range of the tungsten gauge data are below the measured values. This fact suggests that there are some radiators still unaccounted for especially at the lower temperature end of the data. More measurements are needed in the constituent gases of air at various path lengths to answer this question.

Bound-bound atomic transitions could contribute significantly to the air absorption coefficient between 850 Å and approximately 2000 Å. These transitions correspond to electrons in the 2p states of nitrogen and oxygen being excited to higher quantum states. Figure 7 has been drawn to show a general comparison between the free-bound and bound-bound processes for absorption from the ^4S ground state of the nitrogen atom. The absorption cross section is plotted versus wave number. The shaded region is the free-bound contribution assuming a hydrogen continuum oscillator strength for 2p electrons and also that σ varies as $\tilde{\nu}^{-3}$. By the definition of the f-number, the shaded area in the figure divided by πr_o is equal to .19, the Bethe and Salpeter[14] continuum oscillator strength for hydrogen 2p electrons. Assuming hydrogen-like behavior for this state, the remainder of the f-number is in the bound-bound states. This implies that absorption by the nitrogen atom in the ground states could contribute significantly in the wavelength region between 850 and 2000 Å as well as

in the continuum below 850 Å. For an optically thin gas sample or where the lines are strongly broadened, these bound-bound processes could contribute much more to the radiation than the free-bound processes because the transitions occur nearer the black body maximum. For example, the black body curve at 10,000°K integrated from 0 to 2000 Å is 1000 times greater than the integration carried out to 850 Å. The calculation of Bates and Seaton[10] is also shown in Fig. 7 indicating the photoabsorption cross section of 10^{-17}cm^2. This latter cross section was used in making the analysis of the tungsten gauge data.

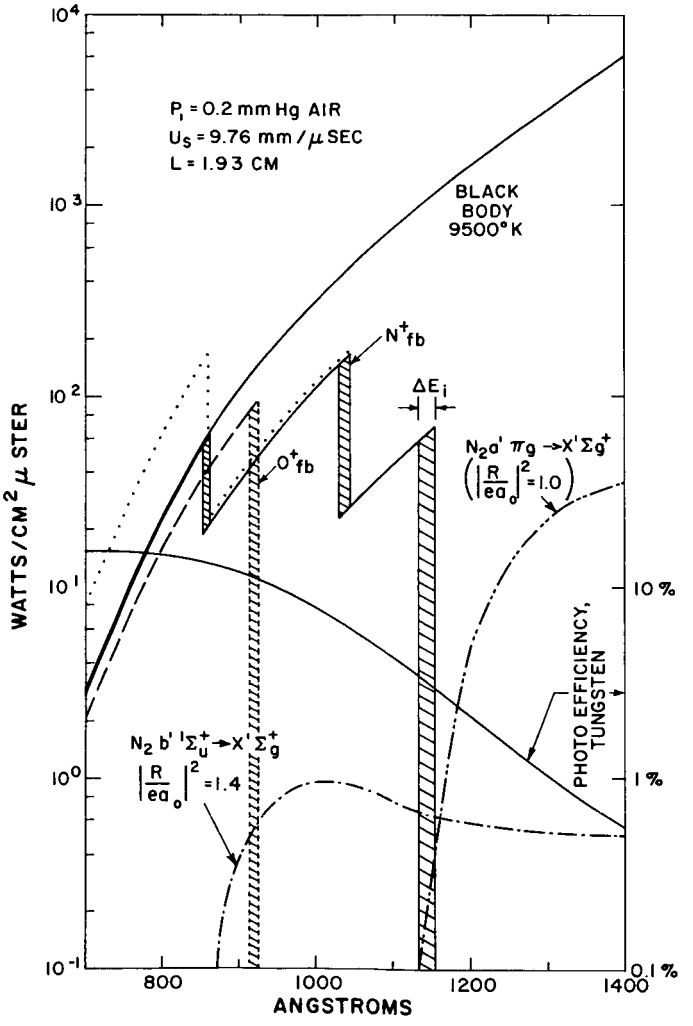

Fig. 6 Radiation contributions to the tungsten photoelectric signal for 9.67 mm/μsec shock condition. The calculation of the various radiators is discussed in the text.

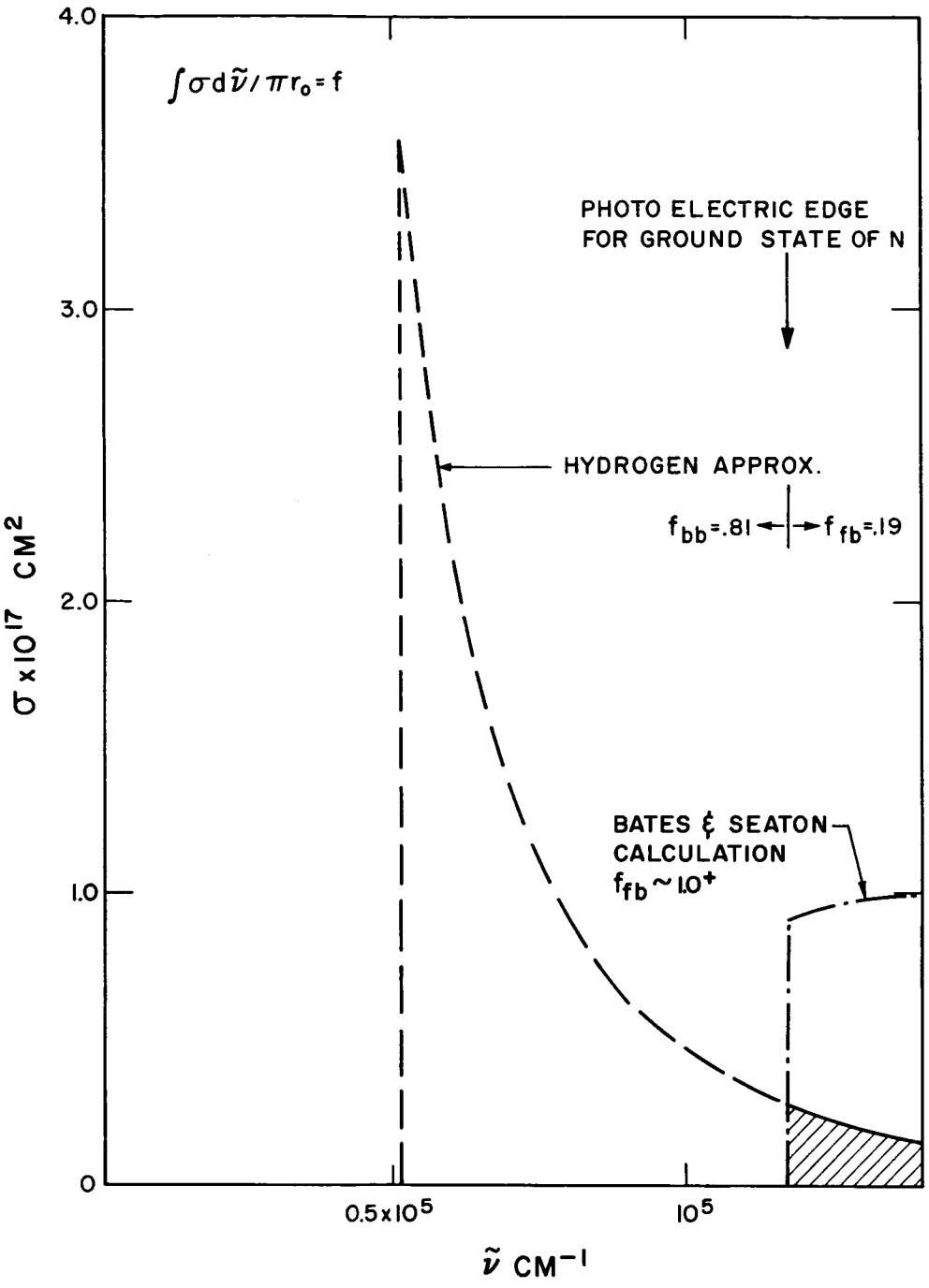

Fig. 7 Diagram showing the wave number distribution of the photo-absorption cross section from ground state of N assuming a hydrogen-like behavior. The figure serves to show how the oscillator strength is distributed over the bound-free and bound-bound transitions.

III. CONTINUUM RADIATION IN THE VICINITY OF 5000 Å

Monochromator Measurements

Photometric measurements of the equilibrium continuum radiation in air, nitrogen and oxygen have been made using standard techniques which are thoroughly described in the literature.[7, 15, 16] A triple channel Jarrel-Ash grating monochromator with photomultipliers and 50 Å resolution in each channel was positioned to observe the radiation in the vicinity of 5000 Å. Photographic spectra show this wavelength region to be relatively clear of line radiation in oxygen and nitrogen shocks. The measurements cover a wide range of density and shock velocity and only part of the data is presented. Figure 8 shows data obtained in air for a 5050 to 5100 Å channel at a constant temperature of 9650°K over a density range which varies by a factor of 200. The highest density data were obtained from reflected shock measurements made looking across the shock about 0.5 cm from the end plate of a cup positioned in the test section. The incident shock measurements were obtained from the equilibrium region produced behind the radiative relaxation region similar to those shown in Fig. 2. Figure 9 shows data obtained in a wavelength channel 4975 to 5025 Å obtained from incident oxygen shocks at a constant initial pressure of 1.0 mm Hg. The range of this data covers a temperature range between 8000 and 12,000°K.

Analysis of the Monochromator Data

Theoretical curves have been constructed in Figs. 8 and 9 which reflect the best estimates for contributions from molecular band and Kramers' radiation. The values for the molecular band f-numbers at the 0, 0 vibrational transition are indicated at the right hand margin of Fig. 8. No internuclear separation dependence was assumed for the electronic transition moment for any of the molecular radiators. The effective Z^2 for the N_{ff} and $N_{2_{ff}}$ are those measured by Taylor[17] at longer wavelengths. The calculation of the O_{fb} contribution in Figs. 8 and 9 is calculated using the photoabsorption cross sections measured by Branscomb and Smith.[18]

The calculation of the N^+ and O^+ free-bound contributions is based on a hydrogen-like model which uses the energy levels for O and N from Moore[11] and the hydrogen continuum oscillator strengths of Bethe and Salpeter[14] for all n states less than 5. A $\tilde{\nu}^{-3}$ dependence is assumed for the photoabsorption cross section. For all other states, the following expression was used for the continuum oscillator strengths[19] with the constraint that $\bar{f}$ must be equal to or less than 1.

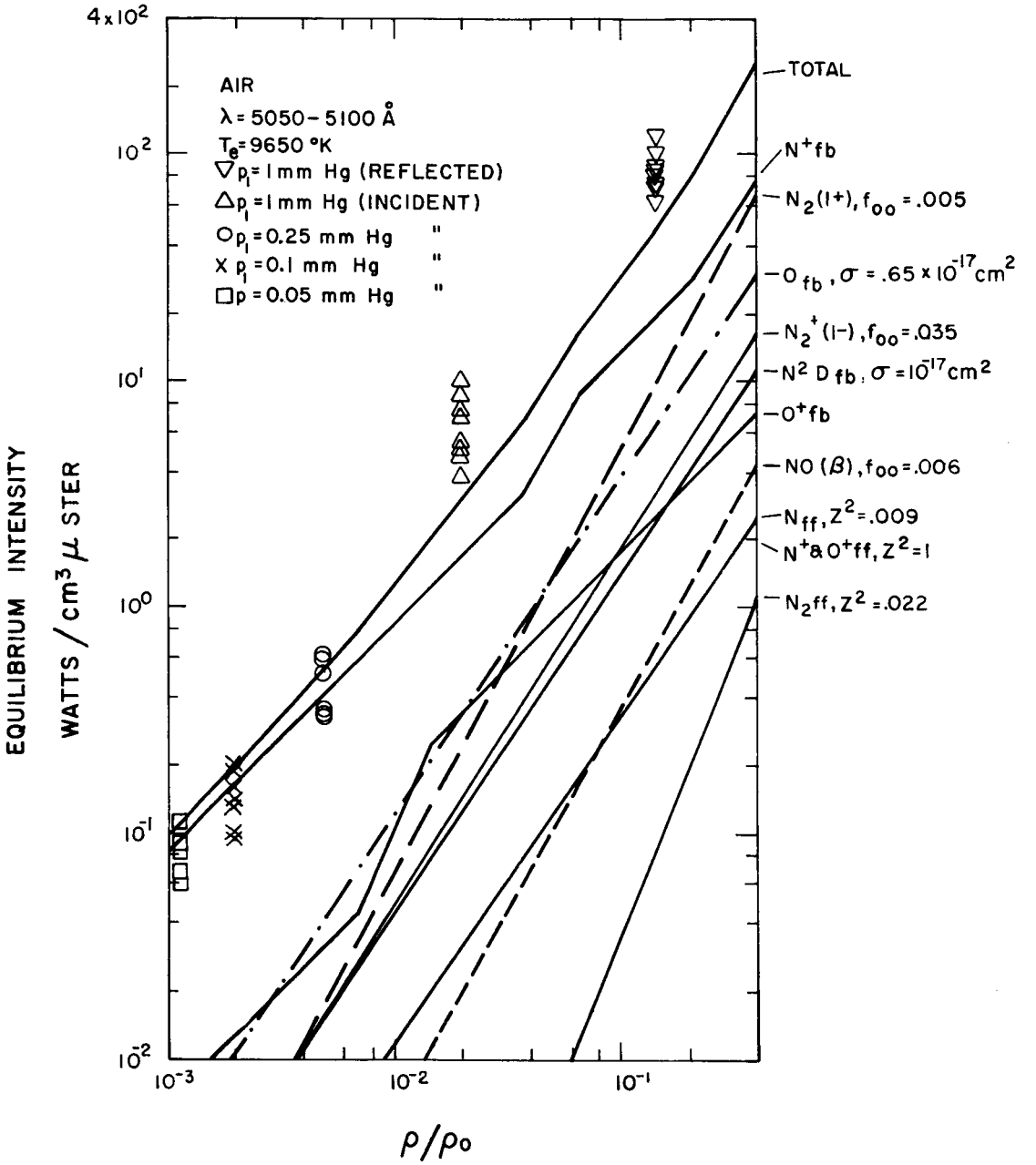

Fig. 8 Photometric measurements of equilibrium air at 9650°K in the vicinity of 5000 Å on incident and reflected shock waves. The pertinent parameters for calculating the various contributors to the radiation are written in the right hand margin. The N^+ and O^+_{fb} calculations are discussed in the text.

A2746

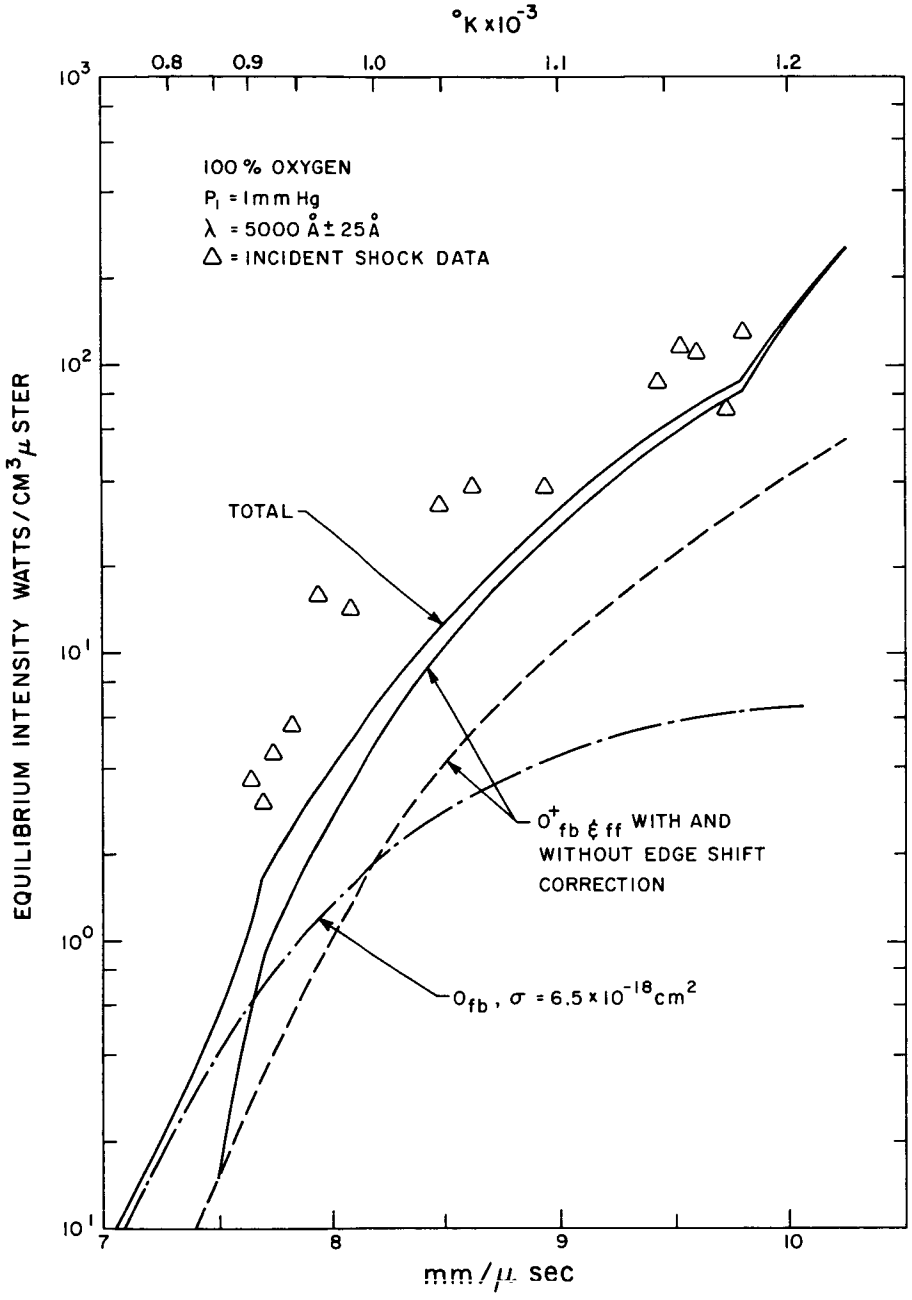

Fig. 9 Photometric measurements of the equilibrium radiation produced behind incident oxygen shock waves at a constant initial pressure of 1.0 mm Hg. The theory lines are discussed in the text.

$$\bar{f} = \frac{16\,R^2}{3\sqrt{3}\,\pi\,\tilde{\nu}_e^2\,(2J+1)n^3}$$

$\tilde{\nu}_e$ is the wave number of the photoabsorption edge for a given state. J and n are the inner quantum and principle quantum numbers, respectively. R is the Rydberg energy expressed in wave numbers. A computer program was used to calculate the free-bound radiation from O^+ and N^+ using the hydrogen assumptions regarding the continuum oscillator strengths. The computer results are shown in Fig. 10 for the N^+ free-bound radiation per total number of N atoms for 9650°K which was the temperature of the data in Fig. 8. Also shown in the figure are the free-free and total radiation using the Unsöld[20] expression with an effective Z^2 of 1. The theoretical curves which are drawn in Figs 8 and 9 for the N^+ and O^+ free-bound radiation also include the effect of the apparent shift of the photoabsorption edges due to the smearing of the high energy levels in the atom. The formulas of Inglis and Teller[12] were used for this edge shift calculation. Since bound-bound transitions have not been included, the N^+ and O^+ free-bound calculations including the edge shift correction should represent a lower limit to the types of measurements displayed in Figs. 8 and 9.

The photoionization cross section, σ, for an atom in a given state, n,ℓ is given by

$$\sigma_{n,\ell} = 2\,\pi\,r_o\,\frac{\tilde{\nu}_e^2}{\tilde{\nu}^3}\,\bar{f}_{n,\ell}$$

where r_o is the classical electron radius. The radiation produced in an optically thin gas sample by electron capture into a given atomic level is then given by

$$\frac{dI}{dV\,d\tilde{\nu}\,d\Omega} = N_{n,\ell}\;\sigma_{n,\ell}\;B_{\tilde{\nu}}\,(1-e^{-hc\,\tilde{\nu}/kT})$$

where $(1-e^{-hc\,\tilde{\nu}/kT})$ is the factor which corrects for induced emission. $N_{n,\ell}$ is the number of atoms in state n,ℓ, $B_{\tilde{\nu}}$ is the black body intensity perpendicular to the surface.

Data similar to that of Fig. 8 was previously used to infer a large contribution to the radiation from electrons being captured to excited nitrogen atoms in the ^2D state. This previous analysis[21] was carried out using the free-bound calculations of Biberman and Norman which are lower than the present hydrogen-like calculations. The observed density dependence was attributed to the interaction of an electron with a neutral atom rather than with an ion. From the present analysis, however, the strong density dependence for the measurements can be explained in terms of a hydrogen-like model for the free-bound radiation and a merging of the lines near photoabsorption edges. For the purposes of the analysis of the

data in Fig. 8, the $N^{-}\,^{1}D$ continuum was calculated using a photoionization cross section of $10^{-17}cm^2$. This value of the cross section was estimated purely on the basis that the photodetachment cross section for O^- measured by Branscomb and Smith was of the order of $10^{-17}cm^2$.

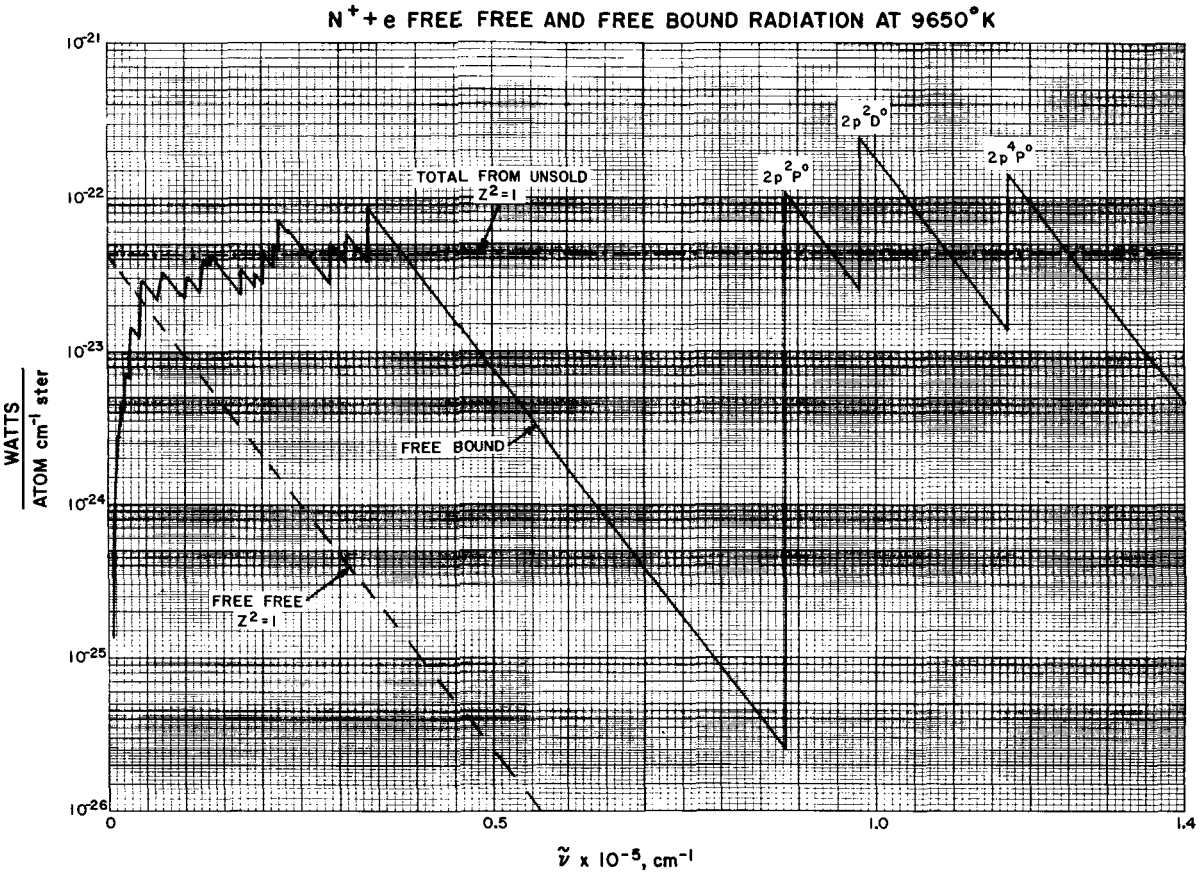

Fig. 10 Free-bound calculations at 9650°K using the hydrogen-like model for the nitrogen atom described in the text. The 2p states are most likely to be in error using this model. An Unsöld calculation for the total and free-free radiation using an effective Z^2 of 1 are also plotted.

IV. INFRARED MEASUREMENTS

Far infrared radiation from a high temperature plasma is predominantly that produced by free-free transitions. Photometric measurements of this radiation on incident air shock waves at a wavelength of 6.1μ were made. A liquid nitrogen cooled gold doped germanium cell was used in conjunction with a long pass filter cutting on at 5μ. A black body cavity was used for the calibration. An optical train consisting of a spherical mirror and optical stops, and a fast response amplifier enabled sufficient spatial resolution to observe the temporal behavior of the infrared signal produced by the radiation behind incident shock waves. Typical data obtained for such measurements are shown in Fig. 11 for two different shock speeds. Time moves from left to right in the figure. The upper trace is produced by the radiation in the visible and shows a small overshoot in the shock front region. For the shock conditions of the data in the figure, the ionization time necessary for the concentration of electrons to equilibrate was about 1 μsec as indicated by both the photomultiplier and infrared cell signals. Equilibrium data obtained between 9 and 13 mm/μsec is shown in Fig. 12. Theoretical curves are calculated for the free-free and free-bound processes which should be dominant contributors over the range of the data. The scattering from neutrals is based on the measurements of Taylor[17] and an effective Z^2 of 1 was assumed for the Kramers' contributions to the radiation. The data points fall about 50% higher than the total theory line indicating an effective Z^2 for the free-free constituents of air of approximately 1.5. Although the nitrogen vibration rotation bands fall in the pass-band of the detector, an estimate of their contribution, based on the work of Breene,[22] shows it to be negligible.

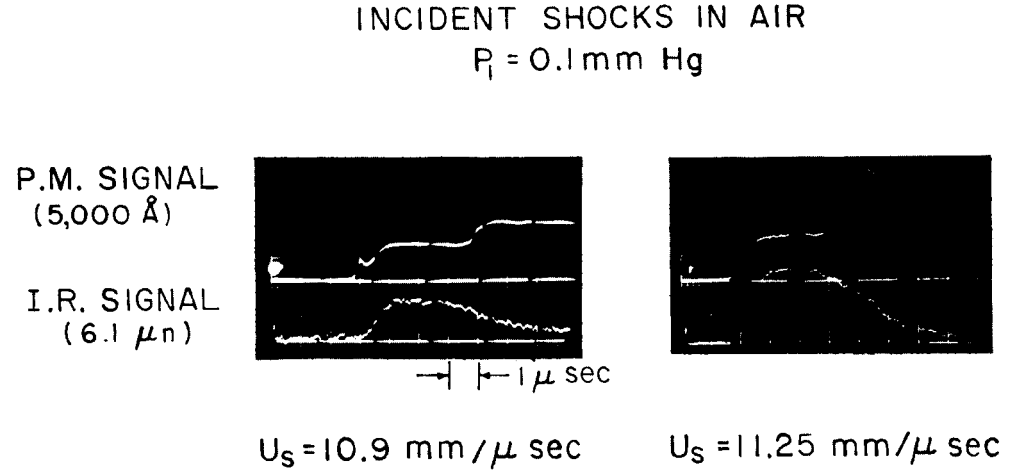

Fig. 11 Typical data obtained at 6.1 μ using infrared cell. The ionization time at the shock front can be seen to be approximately 1 μsec for the indicated shock conditions.

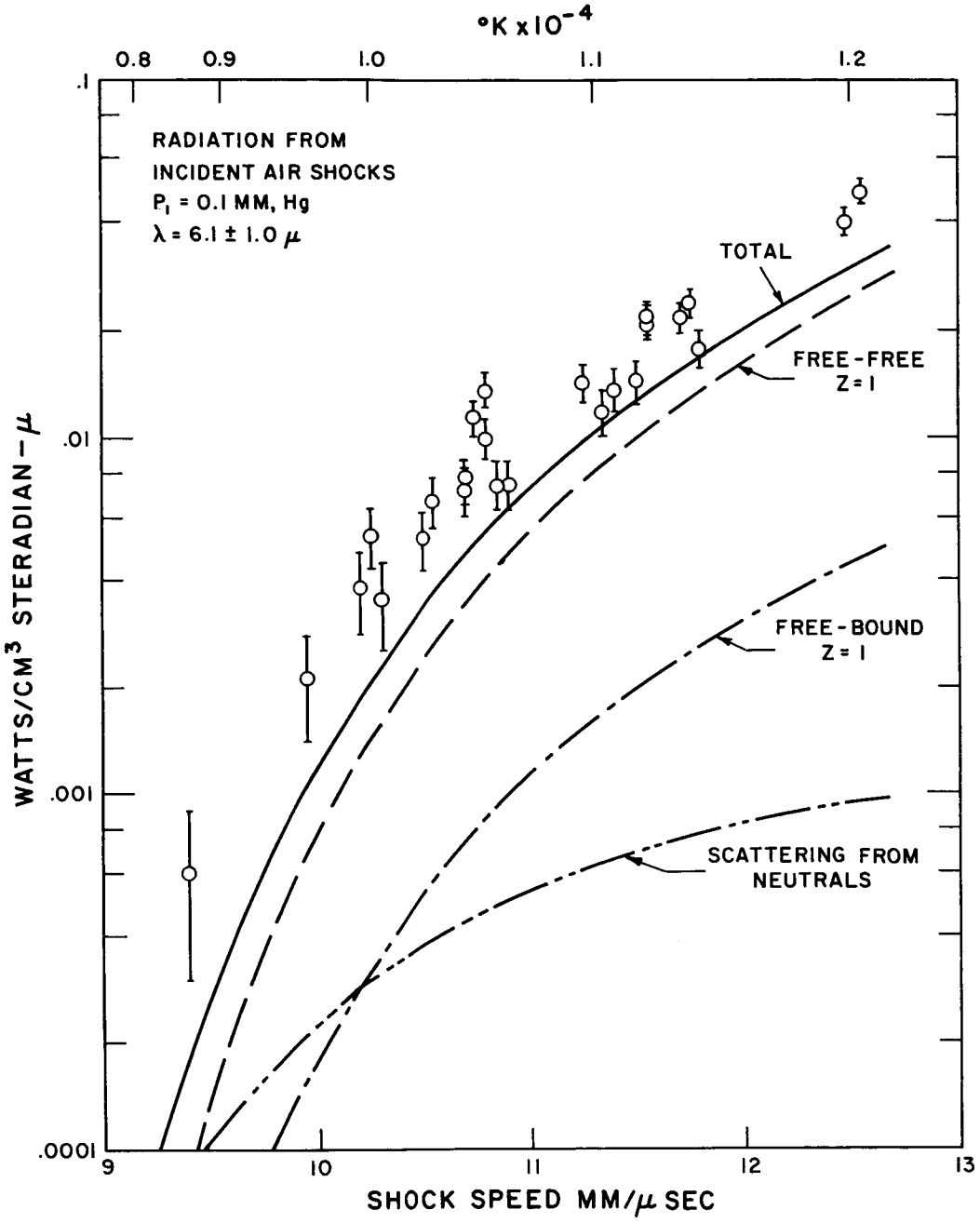

Fig. 12 Equilibrium data of the free-free radiation from air. The data can be used to infer an effective Z^2 or Gaunt factor of 1.5.

V. CONCLUSION

Measurements have been made of the continuum from air and its constituent gases in three spectral regions. The general conclusion is that the hydrogen-like model for free-bound and free-free transitions is reasonably good for all levels other than the 2p states. The measurements in the vacuum ultraviolet are not complete and the indications are that experiments in this wavelength region should be intensively pursued in order to understand bound-bound transitions involving 2p electrons as well as to gain information regarding ultraviolet molecular band systems.

ACKNOWLEDGMENT

Special thanks should be given to J. Camm who designed and built the tungsten gauge, and to R. Spindler of Avco/RAD who kindly provided Franck-Condon factors for the Birge-Hopfield system.

REFERENCES

1. Camm, J.C. and Rose, P.H., "Electric Shock Tube for High Velocity Simulation," Phys. Fluids 6, 663-678, May 1963; also Avco-Everett Research Laboratory Research Report 136, July 1962.

2. Weissler, G.L., Handbuch der Physik, Vol. 21, p. 354. Springer-Verlag, 1956.

3. Weissler, G.L., Handbuch der Physik, Vol. 21, p. 327. Springer-Verlag, 1956.

4. Wray, K.L. and Teare, J.D., "A Shock Tube Study of the Kinetics of Nitric Oxide at High Temperatures," J. Chem. Phys. 36, 2582-2596, May 1961; also Avco-Everett Research Laboratory Research Report 95, June 1961.

5. Keck, J.C., Camm, J., Kivel, B. and Wentink, T., Jr., "Radiation from Hot Air, Part II," Annals of Physics 7, 1-38, May 1959; also Avco-Everett Research Laboratory Research Report 42, February 1959.

6. Keck, J.C., Allen, R.A. and Taylor, R.L., "Electronic Transition Moments for Air Molecules," J. Quant. Spectr. Rad. Transf. 3, November 1963; also Avco-Everett Research Laboratory Research Report 149, March 1963.

7. Allen, R.A., "Nonequilibrium Shock Front Rotational, Vibrational and Electronic Temperature Measurements," Avco-Everett Research Laboratory Research Report 186, July 1964. Presented at the Third National Meeting of the Society of Applied Spectroscopy, Cleveland, Ohio, September 28-October 2, 1964.

8. Patch, R.W., Shackleford, W.L. and Penner, S.S., "Approximate Spectral Absorption Coefficient Calculations for Electronic Band Systems Belonging to Diatomic Molecules," J. Quant. Spectr. Rad. Transf. 2, 263-271 (1962).

9. Wilkinson, P.G. and Houk, N.B., "Emission Spectra of Nitrogen in the Vacuum Ultraviolet," J. Chem. Phys. 24, 528-534, March 1956.

10. Bates, D.R. and Seaton, J.J., "The Quantal Theory of Continuous Absorption of Radiation by Various Atoms in Their Ground States. II. Further Calculations on Oxygen, Nitrogen and Carbon," Monthly Not. Roy. Astro. Soc. 109, No. 6, 698-704 (1949).

11. Moore, C., Atomic Energy Levels, Vol. I. National Bureau of Standards Circular 467, June 15, 1949.

12. Inglis, D.R. and Teller, E., "Ionic Depression of Series Limits in One-Electron Spectra," Astrophys. J. 90, 439-448 (1939).

13. Nicholls, R.W., "Transition Probabilities of Molecular Band Systems XVIII: Franck-Condon Factors to High Vibrational Quantum Numbers I: N_2 and N_2^+," The University of Western Ontario Scientific Report No. 3 under Cont. NONR-2895 (00) and AF 49(638)-640; Scientific Report No. 6 under Cont. AF 19(604)-4560, May 15, 1961.

14. Bethe, H.A. and Salpeter, E.E., Quantum Mechanics of One and Two Electron Atoms. New York, Academic Press, 1957.

15. Allen, R.A., Camm, J.C. and Keck, J.C., "Radiation from Hot Nitrogen," J. Quant. Spect. Rad. Transf. 1, 269-277, December 1961; also Avco-Everett Research Laboratory Research Report 102, April 1961.

16. Allen, R.A., Rose, P.H. and Camm, J.C., "Nonequilibrium and Equilibrium Radiation at Super-Satellite Re-Entry Velocities," IAS Paper 63-77; also Avco-Everett Research Laboratory Research Report 156, September 1962.

17. Taylor, R.L., "Continuum Infrared Radiation from High Temperature Air and Nitrogen," J. Chem. Phys. 39, 2354-2360, November 1963; also Avco-Everett Research Laboratory Research Report 154, May 1963.

18. Branscomb, L.M., Burgh, S.S., Smith, S.J. and Geltman, S., "Photodetachment Cross Section and the Electron Affinity of Atomic Oxygen," Phys. Rev. 111, 504-513 (1958).

19. Aller, L.H., Astrophysics: The Atmospheres of the Sun and Stars. New York, Ronald Press, 1953, pp. 122 and 180.

20. Unsöld, A., Ann. Physik 33, 607 (1938).

21. Allen, R.A. and Textoris, A., "New Measurements and a New Interpretation for High Temperature Air Radiation," Presented at the AIAA Aerospace Sciences Meeting, New York, January 20-22, 1964. AIAA Preprint No. 64-72.

22. Breene, R.G., Jr., "Infrared Emissivity of NO in High Temperature Air," J. Chem. Phys. 29, 512-516 (1958).